A particle-based dissolution model using chemical collision energy

Min Jiang[1], Richard Southern[1] and Jian Jun Zhang[1]
[1]*National Centre for Computer Animation, Bournemouth University, Bournemouth, UK*
{*mjiang, rsouthern, jzhang*}*@bournemouth.ac.uk*

Keywords: Dissolution, Solute, Solvent, Collision Theory, Activation Energy, Particle Excitation, SPH, Erosion.

Abstract: We propose a new energy-based method for real-time dissolution simulation. A unified particle representation is used for both fluid solvent and solid solute. We derive a novel dissolution model from the collision theory in chemical reactions: physical laws govern the local excitation of solid particles based on the relative motion of the fluid and solid. When the local excitation energy exceeds a user specified threshold (activation energy), the particle will be dislodged from the solid. Unlike previous methods, our model ensures that the dissolution result is independent of solute sampling resolution. We also establish a mathematical relationship between the activation energy, the inter-facial surface area, and the total dissolution time — allowing for accurate artistic control over the global dissolution rate while maintaining the physical plausibility of the simulation. We demonstrate applications of our method using a number of practical examples, including antacid pills dissolving in water and hydraulic erosion of non-homogeneous terrains. Our method is straightforward to incorporate with existing particle-based fluid simulations.

1 INTRODUCTION

The reliance of films and games on realistic fluid simulations has led to the popularity of this research topic, with most work in this field focused on the behaviour of fluid itself, such as spray, waves and bubbles (Ihmsen et al., 2012; Cleary et al., 2007; Busaryev et al., 2012) or the interaction with solids (Batty et al., 2007; Robinson-Mosher et al., 2008; Schechter and Bridson, 2012; Akinci et al., 2013). Comparatively few researchers have tackled the challenging problem of the chemical reaction between fluid and solids, which, under the right conditions, can lead to solid mixing with the liquid: a phenomenon known as *dissolution*. The solid in this case is called the *solute* and the liquid is the *solvent*.

Our paper proposes an energy–based dissolution model to describe this complicated fluid–solid interaction. Dissolution is the result of physical and chemical processes: our dissolution model follows *collision theory* which explains how the chemical reaction happens. We introduce a kinetic energy function to measure the particle excitation of the solute, which ensures the same dissolution results even when the object sampling resolutions are different. This approach is advantageous when performing previsualization of the phenomena, allowing animators to quickly preview the dissolution behaviour with a low resolution sampling of the solute.

A solute particle will become dislodged if the local energy exceeds a user specified activation energy. While physically justified, this threshold does not provide a user with an intuition of the total dissolution time. We demonstrate that the activation energy can be approximated as a function of the inter-facial surface area of the solvent/solute and the total dissolution time, providing animators with a tool to more accurately predict the total dissolution rate.

The key contributions of this paper include:

1. a unified particle framework which generates **physically and chemically plausible dissolution behaviour** that is simple to incorporate with an existing particle–based fluid system;
2. an expression for measuring the local particle excitation derived from kinetic energy which is **independent of solute sampling resolution**; and
3. **a mapping between the global dissolution time and local particle excitation** based on the activation energy.

Our particle–based method enables real–time performances using a parallel implementation. We demonstrate plausible dissolution behaviours in different circumstances, such as rotating and translating solids in fluids and pouring fluids onto dissolving objects. Due to the similarity between hydraulic erosion and disso-

lution, our dissolution model is able to simulate erosion without any additional computational overhead.

2 RELATED WORK

The simulation of natural phenomena is one of the most studied areas in Computer Graphics, enabling animators to generate complex and physically plausible dynamics which would be impossible to create manually. We only review work related to dissolution since there is a large body of work in fluid simulation.

In most observable systems, the most frequent solvent is fluid and solute is solid. There have been many studies on the physical interaction between fluids and solids. (Arash et al., 2003) studied the fluid–solid interaction by representing solid with linked point masses. (Batty et al., 2007) applied a pressure projection method with kinetic energy minimization to incorporate irregular boundary geometry into standard grid–based fluid simulations. Their methods are yet difficult to cooperate in dissolution simulation.

(Carlson et al., 2004) and (Amada, 2006) treated the objects as if they were made of fluid. To maintain the object rigidity, (Carlson et al., 2004) identified the object by velocity field, and (Amada, 2006) applied a corrective step to bring back the rigidity of the solid. (Harada et al., 2007) simulated the interaction using collision detection. To prevent fluid particles intersecting the solid boundary, both (Amada, 2006) and (Harada et al., 2007) used penalty force method, which took a few frames to push the particles out. (Becker et al., 2009) also dealt with boundary conditions to ensure no–penetration. However, they required two additional neighbour queries for collision detection, which was expensive to compute.

(Schechter and Bridson, 2012) achieved the no–separation and no–slip boundary condition by sampling the air and solid surface as ghost particles. (Akinci et al., 2012) used corrected density to compute the pressure and viscosity force to avoid the sticking artefacts. Both solved the boundary problem, making an extension to support dissolution simulation. In this paper we use the similar method with (Akinci et al., 2012) to handle the boundary problem during the fluid–solid interaction, but we sample the entire object rather than just the surface since the boundary changes as the shape dissolves.

The methods above tackled the problem of physical interaction between the fluid and solid, but did not consider the chemical interaction between them. Relatively few attempts have been made to simulate the complex chemical reaction between fluid and solid.

(Solenthaler et al., 2007) used an elasticity model for particle–based objects and modelled temperature for phase changes, allowing them to simulate objects melting in hot liquid. (Stomakhin et al., 2014) introduced augmented MPM for phase-change and simulated butter melting in pan. Melting offers a similar visual result with dissolution, but the underlying function is a heat model, which is different from the chemical model in this paper.

(Kim et al., 2010) simulated bubbles around dissolving objects. Their focus was on simulating the dispersed bubble flow — the dissolution model was approximated by generating offsets of a level–set representation of the solute, which had little relationship with actual dissolution behaviour. (Shin et al., 2010) simulated solids dissolving in liquids by modelling solid mass transfer. They treated the solvent and solution as different fluids, and used multiple level–sets to track mixing surfaces which needed to be updated whenever the reactions and interactions occurred — an expensive but necessary step. They also didn't consider about the object separation during dissolution. The latter problem is solved in (Wojtan et al., 2007). However, they both use level–set representation to guide the object surface without additional treatment which means their dissolution results will largely depend on the level-set grid resolution. Furthermore, all these previous approaches did not consider the relationship between the dissolution time and the mass transfer of the solute, meaning that predicting the overall dissolution time is an exercise in trial and error. In this paper we propose a model for predicting total dissolution time from activation energy, and our dissolution model is independent of solute sampling resolutions.

Dissolution also shares many properties with hydraulic erosion. (Beneš et al., 2006) proposed a solution for erosion simulation by using Navier–Stokes equations, while (Wojtan et al., 2007) animated corrosion and erosion by driving the fluids with a finite difference simulation and presenting the solid by advecting the level sets inward. (Krištof et al., 2009) used an SPH based method to simulate erosion, where the erosion model is adapted from an Eulerian approach. The erosion rate used in (Krištof et al., 2009; Wojtan et al., 2007) is derived from the power law, which unfortunately requires a large number of parameters to control, making it impractical for use by an animator. In this paper we demonstrate two practical erosion examples, including one which demonstrates the specification of non–homogeneous solutes forming a natural layering stratum.

3 Dissolution Model

In the following sections we present a model for simulating objects dissolving in fluid, derived from the physics and chemistry behind the solute–solvent interaction. **Collision theory** was firstly proposed by (Trautz, 1916). It describes how chemical reactions take place and why chemical reaction rates differ (McNaught and Wilkinson, 1997). Collision theory is closely related to the kinetic-molecular theory: molecules are in constant motion, occasionally colliding as they move. For a chemical reaction to occur, molecules need to collide in the right orientation and with sufficient energy (Clark, 2004). The energy required for the reaction to occur is referred to as the *activation energy* — necessary to break the existing chemical bonds between substrate molecules.

In our system we volumetrically represent both the solute and the solvent with particles, with each particle becoming a representative component of the corresponding substance. This unified particle representation removes the need for special handling of mixing surfaces. When solute particles collide with the solvent particles, energy is added to the solute particle. Each solute particle carries the energy information which is summed over all the collisions which have occurred. When the energy is larger than a threshold energy—the activation energy—the particle detaches from the object. This activation energy becomes an important factor in determining the dissolution rate. This method allows us to model the dissolution process in a physically and chemically correct manner.

3.1 Solvent representation

Most fluid simulation methods are governed by the Navier–Stokes equations (Foster and Metaxas, 1996). From the viewpoints of the Lagrangian (particle–based) and Eulerian (grid–based) methods, particle–based methods seem to be a natural choice for dissolution because it is easy to implement with arbitrary boundaries and applied forces, while supporting fluid mixing and interaction with arbitrary rigid bodies. Smoothed Particle Hydrodynamics (SPH) was first introduced as a mesh–free Lagrangian method independently by both (Gingold and Monaghan, 1977) and (Lucy, 1977), and is being increasingly used for fluid simulation due to its simplicity. In our model, the physical and chemical reactions between fluid and solid are elegantly simulated by a single SPH solver.

Our method is implemented within the framework of SPH model of (Müller et al., 2003), but is compatible with other SPH models (Ihmsen et al., 2014), such as PCISPH (Solenthaler and Pajarola, 2009), and can be extended with other particle–based representations. We demonstrate the basic SPH model with a short introduction which is required to understand our dissolution method in the following sections. In SPH, a scalar quantity A at location $\mathbf{x}$ is computed by

$$A(\mathbf{x}) = \sum_j m_j \frac{A_j}{\rho_j} W(\mathbf{x} - \mathbf{x}_j, h), \qquad (1)$$

where $W(\mathbf{x},h)$ is a smoothing kernel with smooth core radius h which also decides the neighbourhood size. The kernel satisfies $\int W(\mathbf{x},h)d\mathbf{x} = 1$ and $W(\mathbf{x},h) = 0$ when $\|\mathbf{x}\| > h$. Particle j is the neighbour of the particle at $\mathbf{x}$. m_j is the particle mass and A_j is the field quantity at $\mathbf{x}_j$.

The density and pressure force of the solvent are calculated also based on (Müller et al., 2003). Neighbour searching of the solvent simulation is GPU paralleled using framework of (Hoetzlein, 2014).

3.2 Solute representation

The enclosing volume of the solute is sampled by particles, each of which contributes to the fluid SPH to ensure the correctness of the fluid–solid interaction: (Akinci et al., 2012) and (Schechter and Bridson, 2012) are both good choices for this task. The pressure between the fluid and solid automatically repels the fluid particles and naturally produces the mixing surface with more accuracy at lower computational cost than level–set methods. Since we focus on the dissolution effect when the fluid interacts with the solid, we need to sample the entire object rather than boundary particles to produce the volume change.

For the examples used in this paper, a regular grid sampling is used for the solute. While we have experimented with alternative sampling techniques, but these did not alter our results significantly and are not the focus of this paper.

3.2.1 Sampling Independent Dissolution

Our method ensures the same dissolution result (within error tolerance) even when the sampling resolutions of the solute are different. This property has important applications in computer graphics: for the purposes of pre–visualisation, the dissolution of a lower resolution or adaptively sampled object can be used to predict the behaviour of a very densely sampled object, or simply to improve performance for real–time applications.

In previous methods (Wojtan et al., 2007; Shin et al., 2010) shape alteration of a dissolving object was achieved using mass transfer. Both methods used level–sets to represent the solute, causing the dissolution result to be largely affected by the grid resolution.

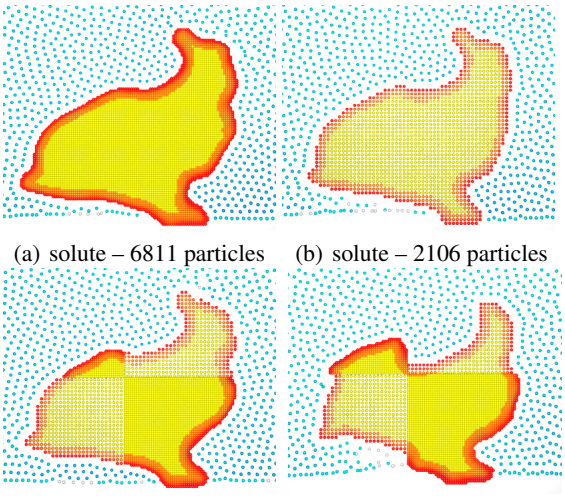

(a) solute – 6811 particles (b) solute – 2106 particles

(c) solute – 4085 particles (d) solute – 4085 particles

Figure 1: 2D bunny dissolving in fluid. Using our method (in (a), (b) and (c)) the sampling density does not affect the dissolution process, even when the sampling is non-homogeneous. In (d) we demonstrate the result when using previous methods (Wojtan et al., 2007; Shin et al., 2010). All the images are taken from the same frame with the same initial conditions. The solute particles with high energy are coloured in red.

In our method we use **volume mass** instead of mass for each solute particle to ensure that our result is independent with the sampling resolution. The volume mass of each solid particle is calculated by

$$m_{vs} = v_s \cdot \rho_s = \frac{V}{N} \sum_j m_s W(\mathbf{x}_s - \mathbf{x}_j, h), \qquad (2)$$

where v_s and ρ_s are respectively the volume and the representative density of each solid particle. V is the volume of the entire object and m_s is the mass of each particle: both of which are constant once the object is initialised. N is the number of particles used to sample the object. It is easy to tell that $\rho_s = \sum_j m_s W(\mathbf{x}_s - \mathbf{x}_j, h)$ originates from the basic SPH density calculation in Equation 1. j is the object particle within the solute neighbourhood h. The volume mass m_{vs} must be updated in each frame due to the changing shape of the object during dissolution.

Figure 1 demonstrates sampling independence by using different sampling resolutions, as well as non–homogeneous sampling resolutions, and compare these against previous dissolution methods (Wojtan et al., 2007; Shin et al., 2010). This property is further discussed in Section 4.2.

3.2.2 Particle excitation

Particle excitation is measured by local particle energy. Since collision itself is a kinetic process, we derive our particle excitation equation from the kinetic energy $\frac{1}{2}m\mathbf{v}^2$, where $\mathbf{v}$ is the *relative velocity*. This is incorporated into Equation 1 to derive an expression for particle excitation:

$$E_s = \frac{1}{2} m_{vs} \sum_f [\frac{m_f}{\rho_f} (\mathbf{v}_l + \mathbf{v}_w + \varepsilon)]^2 W(\mathbf{x}_s - \mathbf{x}_f, h), \quad (3)$$

where m_{vs} is the volume mass from Equation 2; f is the solvent particle within the neighbourhood of solid particle s; m_f and ρ_f are the mass and density of fluid particle; $\mathbf{v}_l$ is the relative linear velocity of solid and fluid particles; and $W(\mathbf{x}_s - \mathbf{x}_f, h)$ is poly6 kernel (Müller et al., 2003), which smooths out the energy according to distance; other kernel may apply, such as cubic spline (Ihmsen et al., 2014).

According to the collision theory, the detachment of particles only occurs when particles collide with right angle and enough strength. In SPH, however, particles cannot collide as they will be repelled by the pressure between particles. Instead, we consider two particles to collide once one particle has entered the neighbourhood of the other. Particles outside of the neighbourhood are not computed. The size of the velocity is affected by the angle of the collision, calculated by:

$$v_l = \max((\mathbf{v}_f - \mathbf{v}_s) \cdot (\mathbf{x}_s - \mathbf{x}_f), 0), \qquad (4)$$

where $\mathbf{v}_{s,f}$ represent the velocity of solid and fluid particles respectively. The direction of $\mathbf{v}_l$ is $\mathbf{x}_s - \mathbf{x}_f$. This is illustrated in Figure 2, where only f_2 and f_3 contribute to the collision.

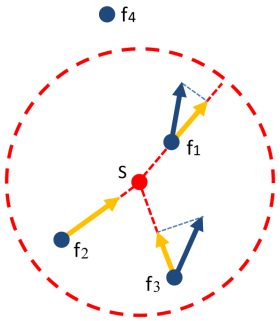

Figure 2: The collision domain. s represents a solid particle and $f_{1,2,3,4}$ are fluid particles. The blue arrows indicate the actual relative velocity, while yellow ones indicate the calculated linear relation velocity $\mathbf{v}_l$.

$\mathbf{v}_w$ represents the angular velocity which contributes to the local particle energy. $\mathbf{v}_w$ is calculated by $\mathbf{w} \times \mathbf{r}$, where $\mathbf{w}$ is the angular velocity and $\mathbf{r}$ is the vector from the particle position to the centre of the object. This is only needed when there is obvious relative rotational motion between the object and fluid.

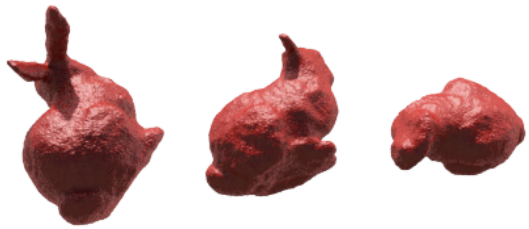

(a) Dissolving without $\mathbf{v}_w$

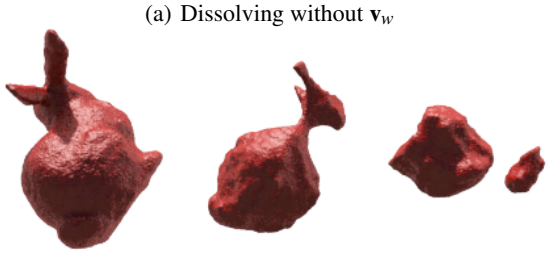

(b) Dissolving with $\mathbf{v}_w$

Figure 3: A spinning bunny dissolves in water. Note that (b) demonstrates separation behaviour (discussed in Section 4.3). The fluid is not rendered in these examples.

Figure 3 shows the different dissolution behaviours of the spinning bunny with and without angular velocity.

A small ε is also added to represent the random thermal motion among molecules ($\varepsilon = 0.00001$ in our model), which gives the possibility of dissolution when there is no macroscopic relative motion between the fluid and solid.

E_s accumulates by time: when it is larger than a user specified activation energy, the particle dissolves into the solution. As described by Equation 2, particles tend to have larger volume mass where the sampling is more compact. This corrects the single particle energy by making the particle more active (i.e. larger energy) in Equation 3, making it dissolve faster.

3.3 Activation Energy

The activation energy provides a physically correct mechanism by which the dissolution rate of individual particle can be controlled. However, this offers no control over the time taken for the object to be completely or partially dissolved: a property that is particularly important to animators seeking to control the simulation without having to resort to trial and error.

In this section we provide the bridge to connect the global dissolution time with the local particle excitation. Dissolution depends on the nature of the solvent and solute, the temperature of both, the inter–facial surface area between them, and the presence of mixing (McNaught and Wilkinson, 1997). In our method the presence of mixing is implicitly solved by the particle excitation. For simplicity, we assume temperature to be a constant parameter θ (although this could be varied within more complex simulations).

We determine the relationship between the total dissolution time T, activation energy E_0 and the inter–facial surface area S based on our simulation experiments. In Figure 4, we show the results of dissolving objects with different inter–facial surface areas and different activation energies. The three objects (sphere, cube, spiky cube) have the same volume. The surface area is respectively 4.83, 6.0, and 8.20.

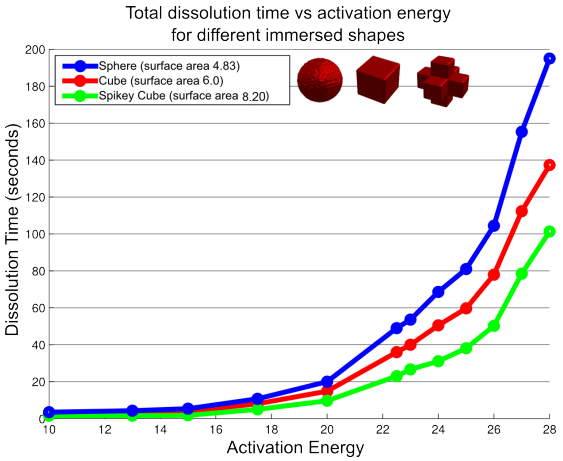

Figure 4: The relationship between the total dissolution time and activation energy for different immersed shapes. Shapes with more surface area in contact with the fluid naturally dissolve faster. The observed dissolution rates leads us to use the exponential function to model the total dissolution time as a function of activation energy.

Each curve describes the dissolution times of certain object with different activation energies. The shape of the curve is best approximated with the general exponential function ($\alpha = 0.25$ in our examples):

$$T \propto \exp(\alpha E_0), \tag{5}$$

By observing the dissolution time of the different objects with the same activation energy, the relationship between dissolution time T and surface area S matches:

$$T \propto \frac{1}{S}. \tag{6}$$

This agrees with common sense: a larger surface area results in shorter dissolution time.

According to Equations 5 and 6, we can conclude that the relationship between the total dissolution time, activation energy and the inter-facial surface area can be described as:

$$T = \frac{\exp(\alpha E_0)}{\theta S}, \tag{7}$$

Using this experimental methodology, artists are able to better estimate the total dissolution time for

objects based on the surface area and the local activation energy. An interactive tool could be developed which uses preceding simulation results of a particular fluid configuration to calculate the coefficients for better estimation. Once the coefficients are determined, the inverse of this function can be used to determine the activation energy for an artist specified target dissolution time.

3.4 Object Update

The positions of solutes are updated as rigid bodies. Each disconnected component will be treated as a rigid body, more detail discussed in Section 4.3. No relative motion is expected among the particles in one rigid body. The forces acted on the object are the forces from the fluid, the gravity, and the support force when the objects hit the boundary. The forces from fluid, such as pressure and viscosity forces, equal to the opposite of the corresponding forces from the object to fluid. The rules updating the solid obey the same with standard rigid body dynamics (Featherstone, 2007).

4 Implementation and Results

We ran our simulations on an Intel Xeon W3680 (8M Cache, 3.33GHz) with 8GB RAM. The SPH fluid simulation implemented in CUDA and executed using a GeForce 460Ti with 1GB onboard RAM. Real–time results are rendered in OpenGL, and simulation results were exported and rendered externally using *Houdini*. The computational cost of our algorithm is depending on the number of both solute and solvent particles, the complexity of interaction between solute and solvent and the update of solute positions. The real–time performance of our technique is presented in Table 1. In a same example, the performance can be largely improved with less solute particles. Therefore, our sampling independent dissolution model allows animators to preview the dissolution behaviour with a lower computational cost. Our method is very efficient and advantageous for pre-visualization.

4.1 Antacid pills to water

Antacid pills are a classic demonstration of dissolution behaviour for simulation. In Figure 5 we demonstrate our effect on two Antacid pills dropped into a glass of water. Bubbles caused by the release of trapped air and chemical processes are recognisable clues that dissolution is taking place. We add bubbles at the dissolution site to increase the authenticity of the simulation. The bubble motion is modelled using basic Brownian motion similar in (Kim et al., 2010).

Table 1: The performance in average frames per second (FPS) of our method in different examples. *Solute* and *Solvent* represent the number of particles in each.

Example	*Solute*	*Solvent*	*FPS*
Spinning bunny	28553	65535	27
Antacid pills	12745	80000	50
Spheres (low)	8538	100000	148
Spheres (high)	22274	100000	48
River Bed	15000	385948	19
Layered Terrain	169650	262140	20

Figure 5: Two antacid pills dissolving in water.

4.2 Sampling Independent Dissolution

In Figure 6 we pour liquid over a sphere, demonstrating the effect of pouring fluid at a targeted area. We also evaluate this example using two different sampling resolutions in order to demonstrating that the dissolution results are equivalent. We calculated the percentage of the volume difference at each frame of both spheres: with our method, this reaches a maximum of 3.4% of the sphere volume, while with the method of (Wojtan et al., 2007; Shin et al., 2010) the low sampled sphere dissolves completely before the high sampled sphere halves in size. The adhesion method of (Akinci et al., 2013) is used to ensure the fluid realistically adheres to the sides of the sphere.

4.3 Separation

During dissolution, parts of object may break off and form separate shapes. In order to track changes to the topology of the shape, we use a region growing algorithm to detect the object separation during dissolution, a method commonly used in image segmentation (Hojjatoleslami and Kittler, 1995). We apply the technique to identify connected regions from amongst the volumetric particles. Particles that are close enough

(a) sphere sampled with 8538 particles

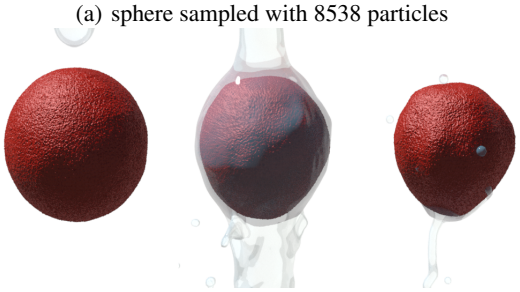

(b) sphere sampled with 22274 particles

Figure 6: Fluid is poured over spheres with different sampling resolutions, with almost identical results, except that the sphere dissolves more smoothly with higher resolution.

are grouped into clusters, each representing a separate rigid body.

The main challenge in implementing this algorithm is testing the proximity of particles, but as we already have neighbourhood information as part of the fluid simulation, this becomes trivial. We update the neighbourhood information before evaluating the region growing algorithm. The region grows from a random seed particle p by adding it to cluster C. Neighbours of p are added to C. Then all new particles in C become the new seeds for the next iteration. Note that only neighbours that are not in C are added. The algorithm proceeds until there are no more valid particles that can be added to C — each resulting cluster is a separate body. Implementing this algorithm in parallel is an interesting area of future research. In Figure 3(b) the bunny separates into pieces as a result of the dissolution.

4.4 Erosion

We use our dissolution method to simulate complex natural erosion phenomena. While we do not use the actual physical properties of different terrain types, these examples demonstrate the viability of using our model for practical simulations. Figure 7 shows the hydraulic erosion acting on the floor of a river bed. As the fluid runs over the terrain, certain soil particles become dissolved in the water. Note that more complex properties of erosion, such as fluid carrying and relocating sediment, are ignored in our simulation.

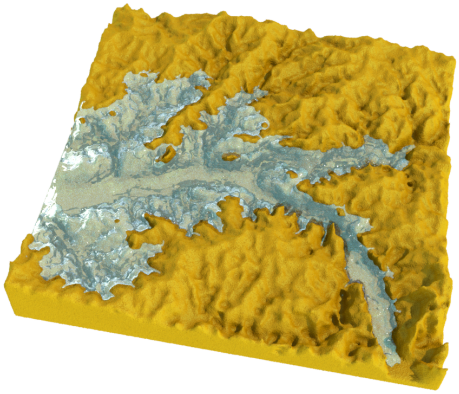

(a) Fluid simulation

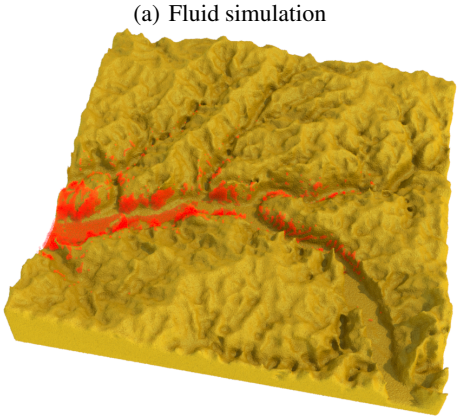

(b) Resulting erosion

Figure 7: Hydraulic erosion with dissolution model. In (a) we show the dissolution process, while in (b) the removed soil particles are shown in red.

One advantage of our energy based model is that we can simulate different terrain types by simply modifying the activation energy of individual layers of particles. This allows us to simulate erosion of rocks consisting of different layers each with different material properties, giving rise to natural formations similar to those which can be found in mountainous or coastal regions.

This is demonstrated in Figure 8, where a three layered terrain is immersed in turbulent fluid to simulate coastal erosion. Different activation energies are assigned to particles in each layer, with the lowest activation energy assigned to the middle layer — leading to a natural arch formation.

5 Conclusion

In this paper we introduce a novel energy-based dissolution model based on the collision theory. We demonstrate by way of examples that this method achieves physically and chemically plausible dissolu-

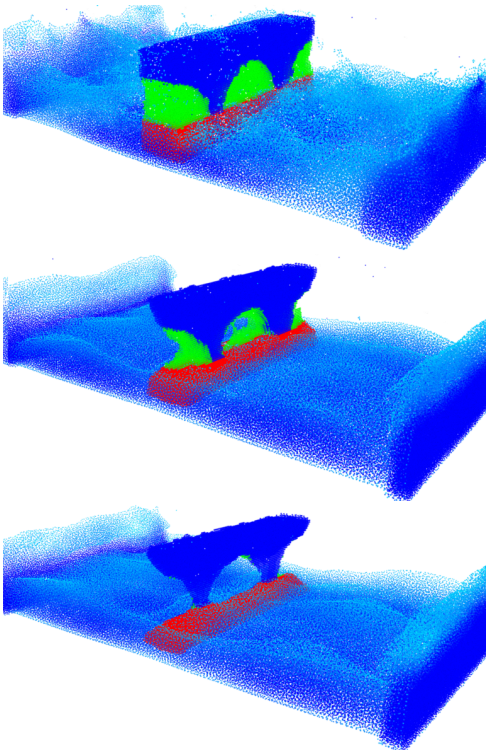

Figure 8: A simulation of layered terrain erosion using our dissolution model. The solute consists of three different material layers, each with a different activation energy. Forces are added to the fluid to keep the fluid active. This simulation consists of about 430k combined particles and runs as 20 frames per second on a commodity graphics card. Please refer to Figure 9 for the rendered results.

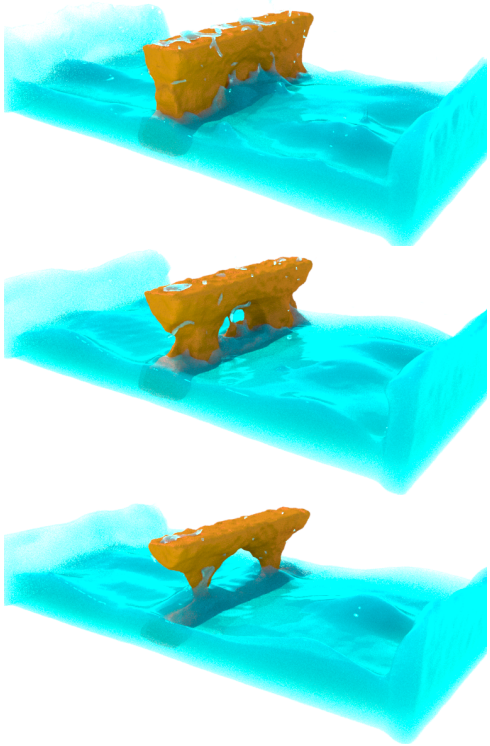

Figure 9: Rendered results of layered terrain erosion using our dissolution model.

tion and erosion behaviours. The key to this model is a new expression for particle excitation based on kinetic energy. By using the volume mass instead of mass to update local particle energy, we are able to ensure the same dissolution results independent of the sampling density.

We also identify the relationship between global dissolution time and the local particle activation energy, allowing animators to easily adjust the global properties of the dissolution simulation by modifying a single parameter. In addition, our method is straightforward to implement in an existing particle–based fluid framework, and naturally lends itself to a parallel implementation.

There are several exciting avenues for research arising from our energy–based model. The independence on sampling resolution implies that adaptively refining solute representations or multi–grid methods could be applied to improve the dissolution computation performance, the incorporation of temperature into our model will allow for more accurate simulation of melting effects, and the unified particle nature of our dissolution model and other recently published work hints at a unified representation for interacting media, allowing gases, solvents and solutes to be simulated within a single framework.

6 ACKNOWLEDGEMENTS

We would like to thank Phil Spicer for fluid rendering, Mathieu Sanchez for providing Signed Distance Field library, Shujie Deng and Wei Wang for video editing.

REFERENCES

Akinci, N., Akinci, G., and Teschner, M. (2013). Versatile surface tension and adhesion for sph fluids. *ACM Trans. Graph.*, 32(6):182:1–182:8.

Akinci, N., Ihmsen, M., Akinci, G., Solenthaler, B., and Teschner, M. (2012). Versatile rigid-fluid coupling for incompressible sph. *ACM Trans. Graph.*, 31(4):62:1–62:8.

Amada, T. (2006). Real-time particle-based fluid simulation with rigid body interaction. In Dickheiser, M., editor, *Game Programming Gems 6*, pages 189–205. Charles River Media.

Arash, O. E., Gnevaux, O., Habibi, A., and michel Dischler, J. (2003). Simulating fluid-solid interaction. In *in Graphics Interface*, pages 31–38.

Batty, C., Bertails, F., and Bridson, R. (2007). A fast variational framework for accurate solid-fluid coupling. *ACM Trans. Graph.*, 26(3).

Becker, M., Tessendorf, H., and Teschner, M. (2009). Direct forcing for lagrangian rigid-fluid coupling. *IEEE Transactions on Visualization and Computer Graphics*, 15(3):493–503.

Beneš, B., Těšínský, V., Hornyš, J., and Bhatia, S. (2006). Hydraulic erosion. *Computer Animation and Virtual Worlds*, 17(2):99 – 108.

Busaryev, O., Dey, T. K., Wang, H., and Ren, Z. (2012). Animating bubble interactions in a liquid foam. *ACM Trans. Graph.*, 31(4):63:1–63:8.

Carlson, M., Mucha, P. J., and Turk, G. (2004). Rigid fluid: Animating the interplay between rigid bodies and fluid. In *ACM Trans. Graph*, pages 377–384.

Clark, J. (2004). *The Essential Dictionary of Science*. New York: Barnes & Noble Book.

Cleary, P. W., Pyo, S. H., Prakash, M., and Koo, B. K. (2007). Bubbling and frothing liquids. *ACM Trans. Graph.*, 26(3).

Featherstone, R. (2007). *Rigid Body Dynamics Algorithms*. Springer-Verlag New York, Inc., Secaucus, NJ, USA.

Foster, N. and Metaxas, D. (1996). Realistic animation of liquids. *Graph. Models Image Process.*, 58(5):471–483.

Gingold, R. A. and Monaghan, J. J. (1977). Smoothed particle hydrodynamics-theory and application to non-spherical stars. *Monthly Notices of the Royal Astronomical Society*, 181:375–389.

Harada, T., Tanaka, M., Koshizuka, S., and Kawaguchi, Y. (2007). Real-time coupling of fluids and rigid bodies. *APCOM in conjunction with EPMESC XI*, (3-6).

Hoetzlein, R. C. (2010-2014). Fast fixed-radius nearest neighbors: Interactive million-particle fluids.

Hojjatoleslami, S. and Kittler, J. (1995). Region growing: A new approach. *IEEE Transactions on Image Processing*, 7:1079–1084.

Ihmsen, M., Akinci, N., Akinci, G., and Teschner, M. (2012). Unified spray, foam and air bubbles for particle-based fluids. *Vis. Comput.*, 28(6-8):669–677.

Ihmsen, M., Orthmann, J., Solenthaler, B., Kolb, A., and Teschner, M. (2014). SPH Fluids in Computer Graphics. pages 21–42.

Kim, D., young Song, O., and Ko, H.-S. (2010). A practical simulation of dispersed bubble flow. In *ACM SIGGRAPH 2010 papers*, SIGGRAPH '10, pages 70:1–70:5.

Krištof, P., Beneš, B., Křivánek, J., and Šťava, O. (2009). Hydraulic erosion using smoothed particle hydrodynamics. *Computer Graphics Forum*, pages 219–228.

Lucy, L. B. (1977). A numerical approach to the testing of the fission hypothesis. *Astron. J.*, 82:1013–1024.

McNaught, A. D. and Wilkinson, A. (1997). *Collision theory*. Oxford: Blackwell Scientific Publications.

Müller, M., Charypar, D., and Gross, M. (2003). Particle-based fluid simulation for interactive applications. In *Proceedings of the 2003 ACM SIGGRAPH/Eurographics symposium on Computer animation*, SCA '03, pages 154–159.

Robinson-Mosher, A., Shinar, T., Gretarsson, J., Su, J., and Fedkiw, R. (2008). Two-way coupling of fluids to rigid and deformable solids and shells. *ACM Trans. Graph.*, 27(3):46:1–46:9.

Schechter, H. and Bridson, R. (2012). Ghost sph for animating water. *ACM Trans. Graph.*, 31(4):61:1–61:8.

Shin, S.-H., Kam, H. R., and Kim, C.-H. (2010). Hybrid simulation of miscible mixing with viscous fingering. *Comput. Graph. Forum*, pages 675–683.

Solenthaler, B. and Pajarola, R. (2009). Predictive-corrective incompressible sph. *ACM Trans. Graph.*, 28(3):40:1–40:6.

Solenthaler, B., Schläfli, J., and Pajarola, R. (2007). A unified particle model for fluid–solid interactions: Research articles. *Comput. Animat. Virtual Worlds*, 18(1):69–82.

Stomakhin, A., Schroeder, C., Jiang, C., Chai, L., Teran, J., and Selle, A. (2014). Augmented mpm for phase-change and varied materials. *ACM Trans. Graph.*, 33(4):138:1–138:11.

Trautz, M. (1916). Das gesetz der reaktionsgeschwindigkeit und der gleichgewichte in gasen. besttigung der additivitt von cv-3/2r. neue bestimmung der integrationskonstanten und der molekldurchmesser. *Zeitschrift fr anorganische und allgemeine Chemie*, 96(1):1–28.

Wojtan, C., Carlson, M., Mucha, P. J., and Turk, G. (2007). Animating corrosion and erosion. In *Proceedings of the Third Eurographics conference on Natural Phenomena*, NPH'07, pages 15–22, Aire-la-Ville, Switzerland, Switzerland. Eurographics Association.